ELSEVIER

Catalysis Today 68 (2001) 97–109

CATALYSIS TODAY

www.elsevier.com/locate/cattod

Preparation of novel uniform mesoporous alumina catalysts by the sol–gel method

Nan Yao [a], Guoxing Xiong [a,*], Yuhong Zhang [a], Mingyuan He [b], Weishen Yang [a]

[a] *State Key Laboratory of Catalysis, Dalian Institute of Chemical Physics, Chinese Academy of Sciences, P.O. Box 110, Dalian 116023, PR China*

[b] *Research Institute of Petroleum Processing SINOPEC, Beijing 100083, PR China*

Abstract

A novel sol–gel process for preparing alumina sol is reported in this article. Ultrasound is used to prepare the alumina sol at room temperature. The study of the effect of ultrasound as a function of treatment time on the pH and the particle diameter distribution of the sol was also made. ^{27}Al NMR, TEM, XRD and DTA were used to detect the properties of the sol and the alumina materials. The result of ^{27}Al NMR shows that there existed Al_{13}^{7+} species in the sol. The acid used not only acted as catalyst for peptizing, but also as reactant to react with aluminum hydroxide to produce the Al_{13}^{7+} species. On the other hand, TEM results show that the morphology of the particles was spherical in the sol, but transformed to needle-like as well as spherical when calcined at 450°C. At the end, the morphology of the particles changed to spherical again at 550°C. By using this alumina sol as precursor, an alumina material with uniform mesoporous distribution was formed after calcination at 550°C without adding any templates or other organic additives. The results of this work also show that the formation of alumina with uniform mesoporous distribution is related to its crystalline phase, the morphology of the particles and the particle diameter distribution of the precursor sol.

Keywords: Sol–gel; Alumina; Uniform; Mesopore; Catalysts

1. Introduction

Most of the shape-selective reactions used by the industry today involve catalysts containing zeolites having pore diameters between 0.5 and 0.6 nm. This size is sufficient to accommodate a broad spectrum of small molecules of technological interest. However, the usefulness of the present-day heterogeneous catalysts in processing high-molecular-weight hydrocarbons, which are of increasing importance, is limited by the pore size of the microporous zeolites used and/or by the pore geometry of the supports. Because of this reason, the demand for mesoporous materials (pore radius higher than 1.0 nm and lower than 25.0 nm) has triggered major synthetic efforts in academic and industrial laboratories [1]. Alumina, mainly in its γ-form, is widely used in catalysis as inert carrier of metal catalysts and as part of bifunctional catalysts, largely because it is inexpensive and reasonably stable, and can provide high surface area for many catalytic applications. As a general rule, the alumina used in catalytic reactions always requires a controlled pore size distribution [2]. Due to the importance of alumina as catalysts, several attempts have been made to synthesize alumina that has uniform mesoporous distribution, which can be applied in the catalytic processing of the large molecules. Compared with the traditional preparation method, the sol–gel process has been proved to be convenient for catalyst carrier synthesis,

* Corresponding author. Fax: +86-411-4694447.
E-mail address: gxxiong@ms.dicp.ac.cn (G. Xiong).

0920-5861/01/$ – see front matter
PII: S0920-5861(01)00296-6

as it is possible to control the pore size and the surface area [3]. Therefore, the sol–gel process is widely used for the preparation of alumina at present. The most often cited process for making alumina sol, the precursor of the alumina materials, developed by Yoldas, is to hydrolyze aluminum *iso*-propoxide or *sec*-butoxide in a large excess of water and in the presence of an acid catalyst in the ratio of 0.07 molar acid/molar Al [4,5]. In this article, we denote this sol–gel preparation route as the Yoldas method. Besides the work of Yoldas, Maeda et al. [6] have shown that the type of solvent to be mixed with aluminum *iso*-propoxide is very important for the final pore size distribution of the calcined alumina. They suggested that the nature of complexation of the alkoxide determined the gel structure, and therefore, the final pore structure. Lopez et al. synthesized γ-alumina from aluminum-*sec*-butylate. They observed a great variation in surface area with the pH in the sol [7]. In the work of Ramsay et al., the precursor alumina sol also could be prepared by peptizing fine powder of boehmite with dilute monoprotic acid [8]. However, the raw materials often used to prepare alumina by the sol–gel method, as reported in the literature and exemplified before, were expensive alkoxides and boehmite powders. Furthermore, the synthesis procedures often have to be carried out at above 80°C in order to avoid the appearance of bayerite that cannot be peptized by acid [9].

In this paper, a novel sol–gel process has been developed. This new method can prepare alumina sol from inexpensive materials such as inorganic aluminum salts. By using ultrasound to provide energy, the temperature of the preparation is successfully controlled at room temperature. Using this alumina sol as a precursor, alumina materials with uniform mesoporous distribution are formed after drying and calcining at desired conditions.

2. Experimental

2.1. Preparation of materials

All the chemicals used in this work were A. R. grade, and the water was deionized and twice distilled. Sufficient ammonium hydroxide (2.5%) was added dropwise to 25 ml of 0.96 M aluminum nitrate solution under vigorous stirring, which brought the pH to about 9.20. The precipitate was collected by centrifugation immediately and then washed by putting it into 50 ml water, and stirred for about 15 min. Washing was continued until the pH of the final suspension was near 7.0. Then a 0.94 M nitric acid was added to this aluminum hydroxide suspension until the desired $[H^+]/[Al^{3+}]$ molar ratio was attained. As soon as the adding of the nitric acid was complete, the beaker which contained the suspension was transferred to the cleaning tank of ultrasonic cleaner, and the cleaning tank was filled with 1.0 l water. After ultrasonic treatment for 10 min, a clear and stable alumina sol was obtained. During the ultrasonic treatment, a thermometer was inserted into the suspension in order to monitor the change of the temperature. After stirred for 10 h, the alumina sol was dried at room temperature in a vacuum box until it began to form white gel. The vacuum box was kept at up to 60 mmHg during the dry procedure. Then the gel was calcined in a muffled oven at 350, 450 and 550°C for 10 h in air, respectively. The appearance of the material is white and hard pieces after drying in vacuum and calcining at 350, 450 and 550°C, respectively. During the whole preparation process, the temperature was strictly controlled at room temperature. The temperature of the sol system would not exceed 40°C even after ultrasonic treatment for 20 min.

2.2. Characterization

The pH of the sol system was monitored using a Cole–Parmer 5986-50 pH meter. The N_4 plus laser scattering particle meter (Coulter) was used to measure the sol particle diameter distribution at 90° to the light beam. A He–Ne laser operating at 10mw was used as the light source. Drops of the sol system were diluted in the sample cuvette with water to give appropriate intensity for the measurement. BET surface area and pore size distribution were determined by N_2 adsorption–desorption at 77 K, using BET, BJH and MP methods, respectively. Measurement was made on an Omnisorp-100CX apparatus from Coulter. All samples were previously desorbed at 300°C under vacuum (10^{-6} Torr) for at least 2 h before recording their isotherms. The phases of all samples were analyzed by powder X-ray diffraction with a Rigaku D/MAX-RB using a copper target at 40 kV and 100 mA. DTA was done on a Perkin-Elmer TDA-1700 instrument in the temperature range of 20–850°C, and

the conditions were: heating rate 5°C/min, air flow 30 cm^3/min. ^{27}Al NMR spectra of solution samples were recorded in a DRX400 (Bruker) spectrometer operating at 104.3 MHz. Chemical shifts were referenced to 1 M $Al_2(SO_4)_3$ solution. The SB2200 commercial ultrasonic cleaner from BRANSON was used as the ultrasound source. The operating frequency of this ultrasonic cleaner is 50 kHz. The sound intensity is 80 W/cm^2. The solvent capacity is 3 l. TEM was performed on a JEM1200EX transmission electron microscope, with a 100 kV accelerating voltage. The sol specimen was diluted to 0.01 M before observation. The solid specimen calcined at 450 and 550°C, respectively; were crushed into powders, embedded in metal copper and polished on both sides of the specimen until the powder was exposed. Then ion etching was performed to make the specimen transparent to electron [10]. In order to keep the original structure of the powder, high temperature treatment and chemicals including acid and base were not used during the specimen preparation for TEM.

3. Results and discussion

3.1. Particle diameter distribution and pH value of the alumina sol

Fig. 1 shows the particle diameter distribution of different alumina sols characterized by the laser light scattering meter. In order to elucidate more clearly, we used the $[H^+]/[Al^{3+}]$ molar ratio to investigate the effect of the acid. As can be seen in Fig. 1, the alumina sols of different concentrations or peptized at different $[H^+]/[Al^{3+}]$ molar ratios all have narrow particle diameter distributions. The result of SDP analysis shows that over 90 wt.% of the particle diameter of every sol was within 20–60 nm. The morphology of the sol particles (0.42 M, $[H^+]/[Al^{3+}] = 0.27$) is directly observed by TEM in Fig. 2. The TEM results reveal that the spherical particles disperse well in this sol system. The results of TEM and laser light scattering measurements imply that alumina sols with good dynamic stability and a narrow particle diameter distribution can be obtained by the procedure proposed.

From the experimental data shown in Table 1, it is evident that the acid concentration also exerted influence on the stability of the alumina sol. The translucent

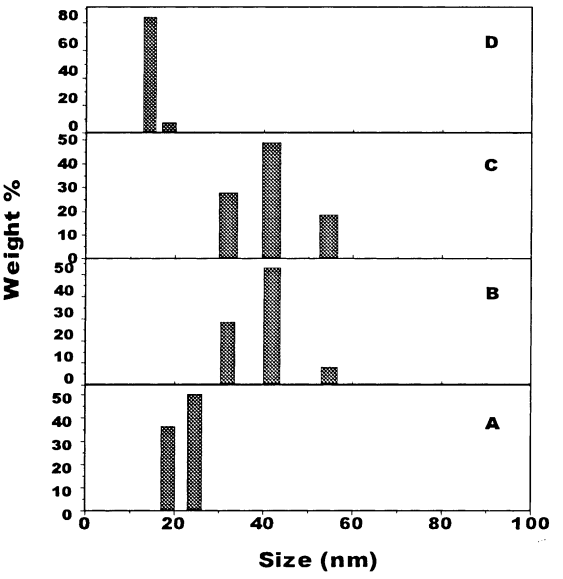

Fig. 1. Particle diameter distribution of the alumina sol. A, B and C indicate the particle diameter distributions of 0.42 M sols peptized at $[H^+]/[Al^{3+}]$ ratios of 0.24, 0.27 and 0.3, respectively; D indicates the particle diameter distribution of 0.12 M sol peptized at $[H^+]/[Al^{3+}]$ ratio of 0.09.

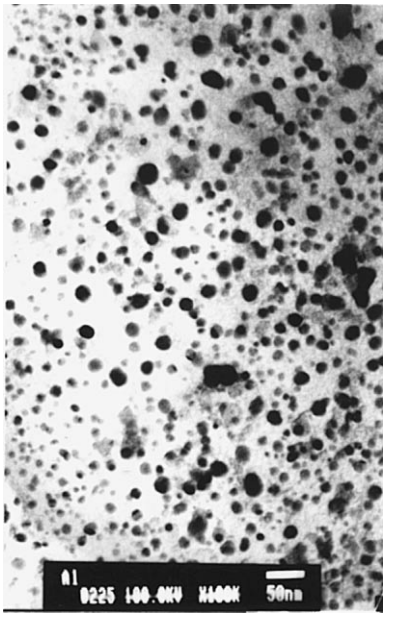

Fig. 2. TEM image of alumina sol obtained by the proposed process.

Table 1
Influence of preparation condition on the qualities of the alumina sol

Sample number	Concentration of $Al(NO_3)_3$ (mol/l)	Concentration of alumina sol (mol/l)	$[H^+]/[Al^{3+}]$ molar ratio	Average particle	
				pH value	Diameter (nm)
A1	0.96	0.42	0.24	4.27	19.2
A2	0.96	0.42	0.27	4.14	35.7
A3	0.96	0.42	0.30	4.17	39.8
A4	0.20	0.12	0.09	4.59	13.6

and homogeneous sol of 0.12 M can only be achieved at $[H^+]/[Al^{3+}]$ molar ratios higher than 0.09, whilst the stable sol of 0.42 M can only be obtained when $[H^+]/[Al^{3+}]$ molar ratios higher than 0.24. This is quite different from the results reported in the literature, where the $[H^+]/[Al^{3+}]$ ratio used was nearly the same for different concentrations of the sols. This ratio was between 0.07 and 0.1 [4]. Furthermore, Table 1 also shows that the sol can be stabilized at higher pH values as compared with the alumina sol of pH value equivalent to 3.6 by the Yoldas method [11]. The interpretation of these strange phenomena will be given in the later section of this article.

3.2. Characterization results of ^{27}Al NMR, XRD and DTA

Before discussing the results further, a few remarks should be made about the crystalline structure and the preparation condition of the Al_{13}^{7+} species. The tridecamer polyoxocation of aluminum $[AlO_4Al_{12}(OH)_{24}(OH_2)_{12}]^{7+}$ has a structure in which the central tetrahedrally coordinated aluminum is surrounded by 12 edge-linked and octahedrally coordinated aluminums. This Al_{13}^{7+} species is often prepared by base hydrolysis of aluminum salts in an aqueous solution at OH/Al ratios of 0.8–2.5 [12,13] (the theoretical OH/Al value for Al_{13}^{7+} is 2.46). In this work, we studied the aluminum species in the sol by ^{27}Al NMR. Several representative ^{27}Al NMR spectra are shown in Fig. 3. Fig. 3A shows the spectrum of the alumina sol that was formed after acid adding and ultrasonic treatment. The sharp peak at 0 ppm in Fig. 3A is attributed to monomer octahedral-Al resonance, and the broad peak centered near 5 ppm is ascribed to oligomer octahedral-Al resonance. The sharp signal at 63 ppm has also been assigned to the tetrahedral-Al and this peak is a significant proof in confirming that the Al_{13}^{7+} species exists in this sol [14]. The spectrum B in Fig. 3 is the ^{27}Al NMR spectrum recorded immediately after the adding of acid to the suspension but without ultrasonic treatment. We can see that the spectra A and B are similar to each other. This result suggests that the Al_{13}^{7+} species appears just after the adding of the acid to the suspension. As can be seen in Fig. 3C, the Al_{13}^{7+} species can also exist in the 0.12 M sample of the alumina sol. Thus, two points of the ^{27}Al NMR results deserve special comment. First, the Al_{13}^{7+} can be prepared by adding a suitable amount of acid to the aluminum hydroxide suspension, besides by base hydrolysis of aluminum salts in aqueous solutions. Another point is that the Al_{13}^{7+} can exist in the alumina sols at room temperature. This one is quite different from the results reported in the literature, such as the work of Olson and coworkers [15,16], which showed that there was no Al_{13}^{7+} species in the alumina sol.

The crystalline phase of the gel that was carefully dried in vacuum at room temperature is also shown in Fig. 4. In this XRD pattern, the dominant phase is pseudoboehmite, also called gelatinous boehmite, which has a water content of 1.3–1.8 mol H_2O:1 mol Al_2O_3, as compared with the 1:1 ratio observed in boehmite. Thus, pseudoboehmite has an X-ray diffraction pattern which is similar to that of boehmite. In order to confirm the XRD result, we conducted DTA analysis. The DTA profiles are also illustrated in Fig. 4 for the gel and the pure boehmite samples, respectively. In the DTA curve of the gel sample, an endothermic peak is observed at 250°C and can be ascribed to crystal transformation from pseudoboehmite to γ-Al_2O_3. As for the pure boehmite sample, the 450°C endothermic peak is attributed to the transformation of boehmite to γ-Al_2O_3 [2,17]. The results of the DTA analysis testify that the gel phase is essentially pseudoboehmite. Therefore, in the preparation

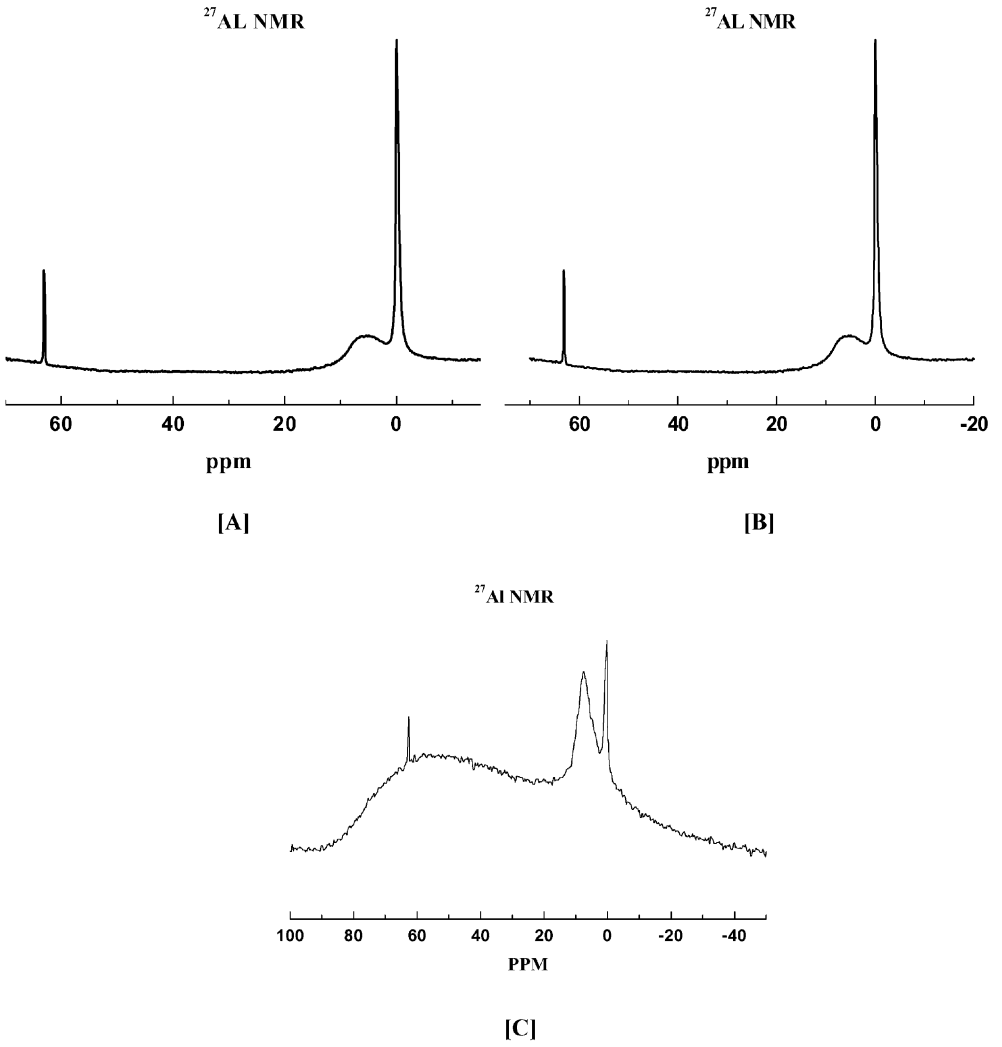

Fig. 3. ^{27}Al NMR spectra of different samples. (A) The spectrum of 0.42 mol/l sol peptized at $[H^+]/[Al^{3+}]$ ratio of 0.27; (B) the spectrum recorded just after the adding of the acid, but no ultrasonic treatment; (C) the spectrum of 0.12 mol/l sol peptized at $[H^+]/[Al^{3+}]$ ratio of 0.09.

method proposed in this article, the transformation of pseudoboehmite to bayerite at room temperature is hindered.

3.3. The effect of ultrasonic treatment

As mentioned before, the alumina sol is often prepared from alkoxides at temperatures higher than 80°C. The reasons why this procedure should be carried out at above 80°C are: (1) cold-water hydrolysis forms pseudoboehmite that transfers to bayerite upon aging through a dissolution–recrystallization process, and the bayerite cannot be peptized by acid due to the large crystal size [9], and (2) a higher temperature can provide certain energy to break down the weak bonds that cause aggregation between the particles. In recent years, ultrasound has been found many new applications in chemistry. According to the article on this subject, ultrasound provides a form of energy which can modify the chemical reactivities in different ways,

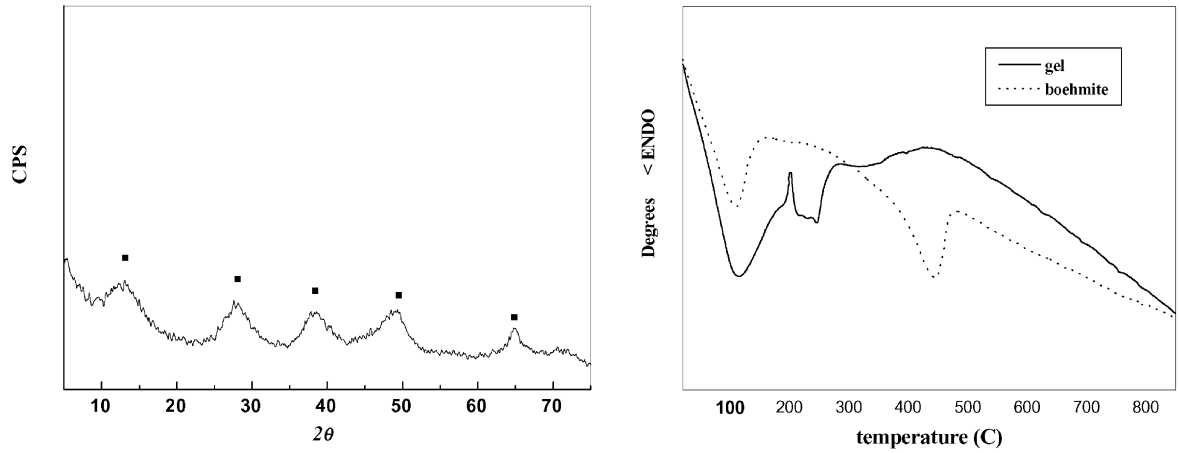

Fig. 4. The XRD pattern of the gel dried in the vacuum and DTA curves of the gel and the pure boehmite sample. The solid line curve is the gel, and the dot line is the boehmite.

as comparing with other conventional energy sources such as heat, light or pressure [18]. Combining with the concepts shown before, our attention is drawn on the possibility of utilizing ultrasound to replace heat in the preparation of alumina sol, so that the operating temperature can be controlled below 80°C. The results shown in Fig. 1 and Table 1 have actually indicated that the stable sol which has narrow particle diameter distribution can be obtained by using ultrasound in this work. As far as we know, this is the first report on the preparation of stable alumina sols below 80°C.

In general, the effect of ultrasound includes heat effect, mechanical effect and other effects. In this experiment, the temperature of the sol system was measured during the ultrasonic treatment. The result showed that it was not higher than 40°C after the ultrasonic treatment 20 min. Therefore, the heat effect is not a main factor in this study. As discussed before, the $Al_{13}{}^{7+}$ species appears just after the adding of the acid. Thus, the effect of ultrasound in this work does not cause the occurrence of a chemical reaction. What is the main effect of the ultrasound in this study? From detailed calculation, we can answer this question.

Using SB2200 ultrasound instrument, with $f = 50\,\text{kHz}$, $I = 80\,\text{W/cm}^2$, $C = 1500\,\text{m/s}$, $\rho = 1000\,\text{kg/m}^3$, we have

$$P_A = (2\rho CI)^{1/2} = 1.549 \times 10^6 \quad (1)$$

$$v_0 = \frac{P_A}{\rho C} = \frac{1.549 \times 10^6}{1500 \times 1000} = 1.033 \quad (2)$$

$$a_0 = \frac{dv}{dt} = 2\pi f v_0 = 3.24 \times 10^5 \quad (3)$$

where C is the transmission velocity of sound in water, I the sound intensity, v_0 the maximum velocity of the particles (in m/s), ρ the density of water, f the frequency of ultrasound, a_0 the maximum acceleration of the particles (in m/s^2), and P_A the sound pressure (in N/s^2).

The calculation result shows that the maximum acceleration of the particles is $3.24 \times 10^5\,m/s^2$ during the ultrasonic treatment under the experimental condition [19]. This value is 3.3×10^4 times as much as the value of gravity acceleration. Thus, the ultrasonic treatment can provide enough energy to break down weak bonds that cause particle aggregation at room temperature, as compared with the mechanical stirring.

In this study, although the suspension has already been peptized to small particles after the adding of the acid, a translucent and homogeneous sol is not formed, because most of the small particles aggregated together. The weak bonds such as van der Waals force are the main reason that cause this aggregation at room temperature. Since enough energy can be provided by the ultrasound, as calculated previously, the ultrasound applied immediately after the adding of the acid

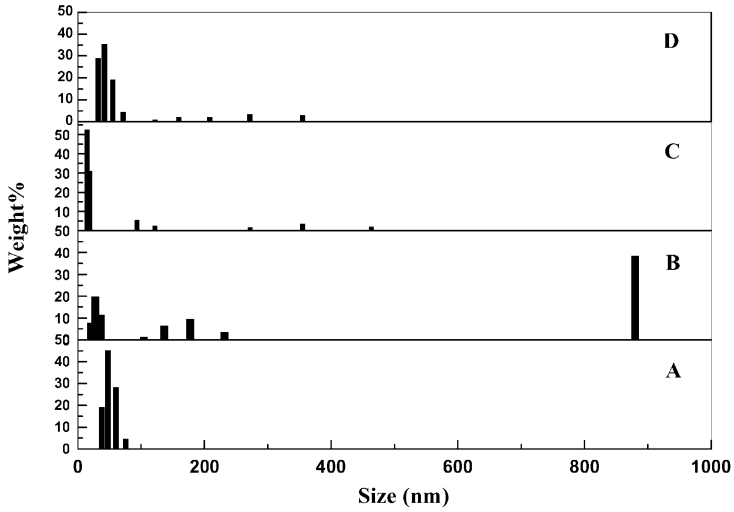

Fig. 5. Particle diameter distribution of alumina sols treated by ultrasound for different time and measured immediately. (A) Treatment by ultrasound for 10 min; (B) treatment by ultrasound for 13 min; (C) treatment by ultrasound for 16 min; (D) treatment by ultrasound for19 min.

can smash the weak bonds to form a stable sol system. Therefore, the dissolution–recrystallization process that caused the transformation of pseudoboehmite to bayerite is hindered, because the pseudoboehmite particles are protected by the double layer of the sol. In summary, in this study, ultrasonic treatment is one of the important factors for preparing alumina sols at room temperature from inorganic salts.

Fig. 5 shows the effect of ultrasonic treatment on particle diameter distribution of the sol. In Fig. 5, we can see that the particle diameter distributions measured by the laser light scattering meter are dissimilar after ultrasonic treatments for 10, 13, 16 and 19 min, respectively. The large particles appearing after treating for 13, 16 and 19 min, together with the smaller particles, can also be observed by comparing Fig. 5B and C with Fig. 5A. The change tendency of the pH value is shown in Fig. 6. We can see that the pH value decreases with the increase of treatment time. A possible explanation of these phenomena is the agitation of the double layer of the sol by ultrasound. The steady double layer structure of the sol particles has already been formed after ultrasonic treatment for 10 min. Further treatment will destroy this double layer again. Some protons will desorb from the particles to the solution and cause a decrease of the pH value. Thus, the stability of the sol particles is broken. Large agglomerates can then be regenerated due to the inter-particle contact, and a broad diameter distribution is therefore formed. In another way, the smaller particles can also be obtained by ultrasonic treatment for a longer time. But this system is unstable, and the large agglomerates will precipitate. The experimental results shown in Figs. 5 and 6 suggest that ultrasonic treatment has a great influence on the pH value and the particle diameter distribution of the sol. Fig. 7 shows the particle diameter distribution of the sol that was treated by ultrasound for 10 min but measured at different time. Plot A in Fig. 7 shows the particle diameter distribution measured just after the treatment, while plot B in Fig. 7 shows the particle diameter distribution measured 1 year later. By comparing these two plots, it is evident that the particle diameter distribution had not changed after 1 year. This result suggests that 10 min is the best ultrasonic treatment time.

3.4. The formation mechanism of the alumina sol

As discussed in Section 3.1 of this article, the $[H^+]/[Al^{3+}]$ ratios used to prepare alumina sols under different concentrations are not identical, and the alumina sols can be stabilized under the condition of higher pH values. In an attempt to provide an answer to these strange phenomena, a new formation

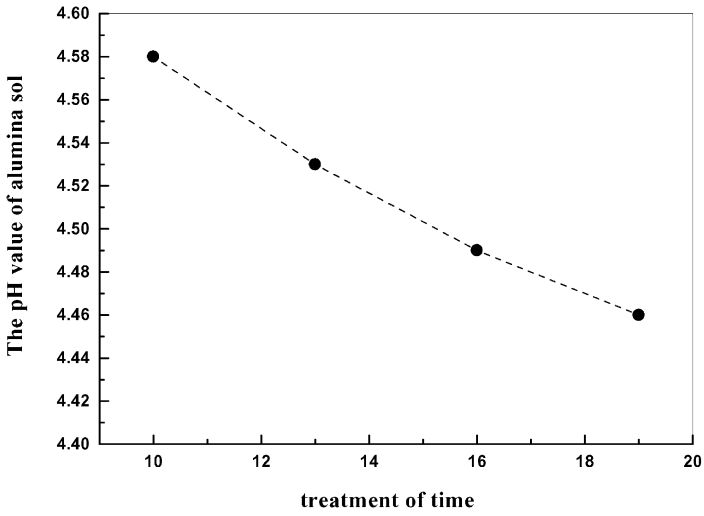

Fig. 6. The relationship between the pH value and the treatment time.

mechanism of the sol has been suggested based on the results of ^{27}Al NMR and XRD characterization.

The precipitate was formed after adding sufficient ammonium hydroxide to the aluminum nitrate solution. After washing for several times, the pH value of the suspension was near 7.0. Under this condition, amorphous aluminum hydroxide and pseudoboehmite were the main components in the precipitate, as reported in the literature [20]. Then a certain amount of acid was added to this suspension. According to the results reported by Ono et al. [20], both these amorphous aluminum hydroxide and pseudoboehmite were stable at alkaline condition, but the amorphous aluminum hydroxide would readily dissolve in acid, while the pseudoboehmite would not. So part of the acid would react with the amorphous aluminum

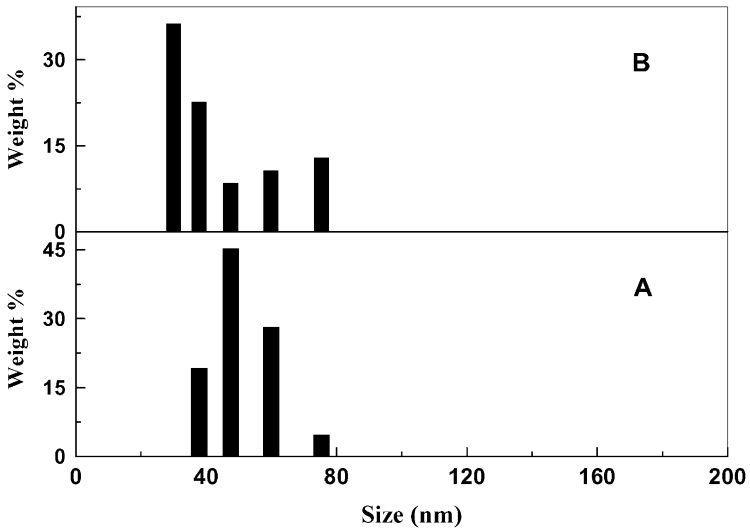

Fig. 7. The particle diameter distribution of the alumina sols treated by ultrasound for 10 min and measured at different times. (A) Measured just after treatment; (B) Measured 1 year after treatment.

hydroxide to form the Al_{13}^{7+} species. We define this part of the acid as $[H_1^+]$. Eq. (4) shows this reaction:

$$13Al(OH)_3 + 7H^+ + H_2O \rightarrow [AlO_4Al_{12}(OH)_{24}(OH_2)_{12}]^{7+} \quad (4)$$

The results of ^{27}Al NMR in Fig. 3 have already indicated this aspect. But another part of the acid was used as a catalyst [2] to peptize the pseudoboehmite suspension in the precipitate to form smaller particles, and we define this part of the acid as $[H_2^+]$. Actually, these two reactions occur at the same time. In fact, the $[H^+]/[Al^{3+}]$ molar ratio used can really be written as $\{[H_2^+] + [H_1^+]\}/\{[\text{pseudoboehmite}] + [\text{amorphous aluminum hydroxide}]\}$. Thus, it is reasonable to believe that the acid used is not only to peptize but also to react with the hydroxide to produce Al_{13}^{7+} species. This is the first time to report that the acid used in the preparation of the sol has two functions. A stable sol was formed after ultrasonic treatment, as has been discussed previously. The whole formation mechanism of this alumina sol suggested by us is illustrated in Fig. 8.

Because the acid has two functions, it is easier to understand why the $[H^+]/[Al^{3+}]$ ratio used to prepare the alumina sol under different concentrations is not identical. If the concentration of the aluminum nitration solution is different, the content of amorphous hydroxide and the pseudoboehmite in the precipitate are also different. Then the $[H_1^+]$ used to react with the hydroxide will be dissimilar. But in another way, the $[H_2^+]$/[pseudoboehmite] ratio used is similar because $[H_2^+]$ is used just as a catalyst for peptization. Consequently, the $\{[H_2^+] + [H_1^+]\}/\{[\text{pseudoboehmite}] + [\text{amorphous aluminum hydroxide}]\}$ ratio (the $[H^+]/[Al^{3+}]$ ratio) used is not the same in preparing the sol with different concentrations.

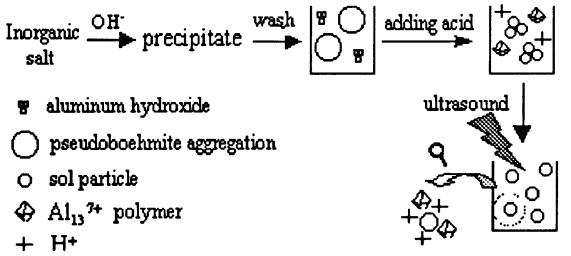

Fig. 8. The alumina sol formation mechanism.

Because some part of the acid was consumed to react with the amorphous hydroxide for producing the Al_{13}^{7+} species, it is rational to find that the pH value of this alumina sol is higher than the value reported in the literature. As is well know the stability of the sol is mainly due to the inter-particle electrostatic repulsion. However, some excellent work done by Ramsay et al. [8] showed that there is another short-range repulsion force which can arise from the presence of polymeric aluminum cations in colloidal systems. In this work, the result of ^{27}Al NMR has already proved the existence of the Al_{13}^{7+} species. Thus, it is reasonable to suggest that some of the Al_{13}^{7+} polymers adsorbed on the sol particles can provide a short-range inter-particle repulsion. In addition to the inter-particle electrostatic repulsion, this short-range inter-particle repulsion can also provide an extra force that makes the sol particles to become stabilized at higher pH values.

3.5. The surface area and pore size distribution of alumina materials

The 0.42 M precursor sol peptized at the $[H^+]/[Al^{3+}]$ ratio of 0.27 was dried according to the proposed method and calcined at different temperatures to obtain various crystalline phases of alumina. An experimental study of the adsorption and desorption branches of the nitrogen isotherms was carried out for these alumina samples. Fig. 9 shows the plots of the isotherms of the samples calcined at 350, 450 and 550°C, respectively. As can be seen in Fig. 9, nos. 1 and 3 are I + IV type adsorption isotherms, but no. 2 is a typical IV type adsorption isotherm. The H2 type hysteresis loops are observed in all cases, thus indicating the existence of the mesoporous texture. In the relative pressure range between 0.05 and 0.25, the experimental data can be fitted with excellent agreement to the well-known BET equation (linear correlation better than 0.999). The specific surface area data of the samples calculated by the BET equation is shown in Table 2. The surface area of the sample is 178.57 m^2/g at 350°C and 265.72 m^2/g at 450°C. When the temperature rose to 550°C, this value decreased to 158.37 m^2/g.

Another feature of this alumina is its pore size distribution. Considering that the BJH method is only used to calculate the mesopore distribution from the

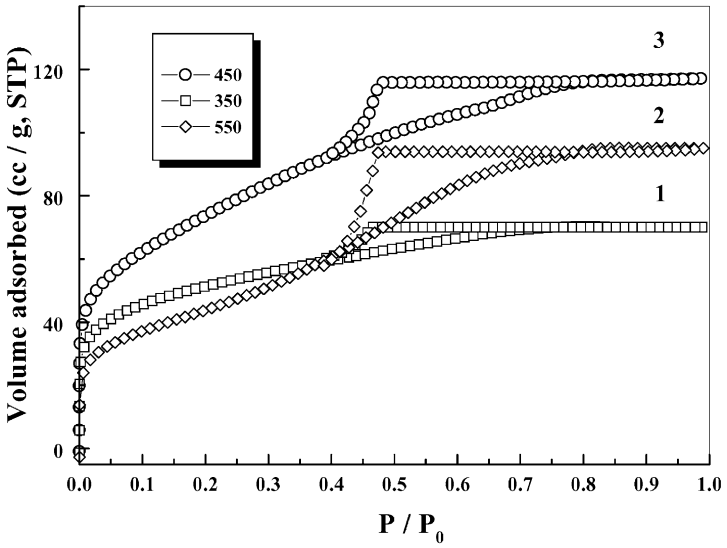

Fig. 9. Adsorption–desorption isotherm plots of aluminas calcined at different temperatures of: (1) 350°C; (2) 550°C; (3) 450°C.

desorption isotherm, the MP method which is an extension of the *t*-plot procedure was applied to calculate the micropore distribution from the adsorption isotherm [21]. The calculation results in Table 2 show that micropores and mesopores existed together in aluminas calcined at 350 and 450°C. But micropores disappeared entirely and there was only mesopore in alumina after calcined at 550°C. Fig. 10 shows the pore size distribution of the alumina at 550°C, as calculated by the BJH method. In Fig. 10, the alumina sample gives a single maximum in its distribution, centering around 3.6 nm. In order to check the existence of microporosity in this sample, the MP method is used again to calculate the micropore distribution from the adsorption isotherm. The result suggests

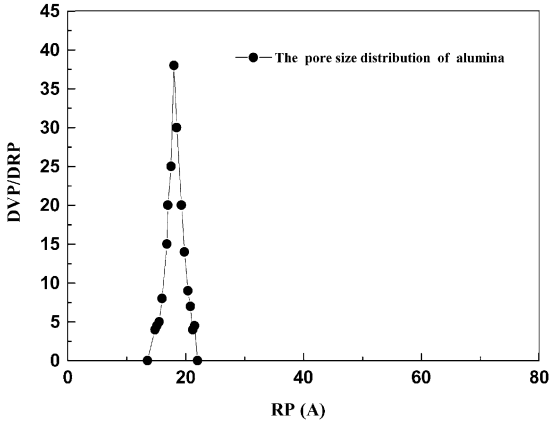

Fig. 10. Pore size distribution of the alumina calcined at 550°C.

Table 2
Influence of calcination temperature on the texture of the sample

Temperature (°C)	Specific surface area (m^2/g)	Pore volume (ml/g)		Pore size distribution (nm)	
		Micropore	Mesopore	Micropore	Mesopore
350	178.57	0.098[a]	0.044[b]	1–1.8[a]	3–4.0[b]
450	265.72	0.159[a]	0.080[b]	1.3–2[a]	3.5–4[b]
550	158.37	–	0.13[b]	–	2.8–4.2[b]

[a] Calculated from adsorption isotherm by the MP model.
[b] Calculated from desorption isotherm by the BJH model.

that, according to this method, no microporosity can be detected in this sample. In most cases, the mesoporous alumina was prepared by using templates to form and adjust the pore size [22,23]. The results shown in Fig. 10 and Table 2 imply that the alumina with uniform mesoporous distribution and large surface area can be prepared by using this alumina sol as a precursor and after calcined at 550°C, without using any templates.

In order to investigate the phase transformation and the relationship between the pore size distribution and the crystalline phase, powder XRD patterns were recorded as a function of the calcination temperature. Fig. 11 shows the X-ray powder diffraction patterns of the samples calcined at different temperatures. As can be seen from Fig. 11, the initial phase is pseudoboehmite. Then this pseudoboehmite began to disappear after calcined at 350°C. Subsequently, γ-Al_2O_3 appeared at 450°C and this γ-Al_2O_3 phase was completely formed when the temperature increased to 550°C. The morphology of the alumina particles calcined at 450 and 550°C, respectively, was also detected by TEM, and Fig. 12 shows these TEM images. It is obvious that needle-like and spherical particles co-exist in picture A of Fig. 12, but there are only pure spherical particles in picture B. This results indicate that the particle morphology changes during the heat treatment. Combining with the results of the TEM and XRD, we know that the needle-like particles are pseudoboehmite and the spherical particles are γ-alumina. When the temperature was increased

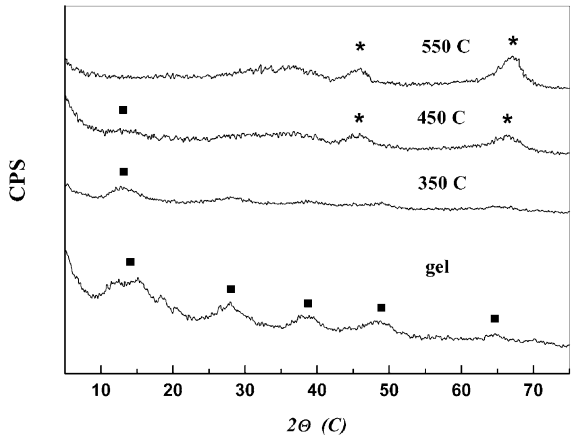

Fig. 11. XRD patterns of pseudoboehmite gel and alumina calcined at 350, 450 and 550°C, respectively. (■) pseudoboehmite; (*) γ-Al_2O_3.

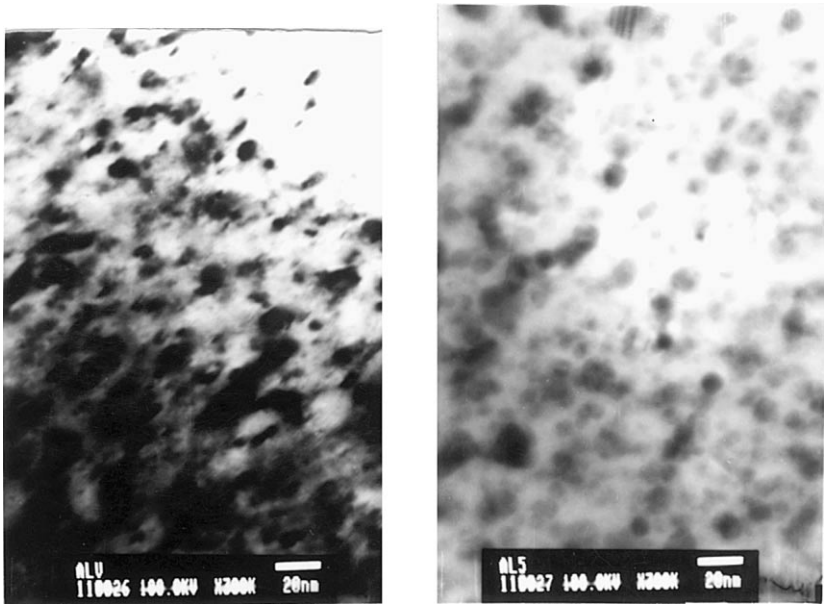

Fig. 12. TEM image of the alumina obtained by calcining at 450 and 550°C, respectively. (A) 450°C; (B) 550°C.

to 550°C, the needle-like pseudoboehmite particles disappeared, so that there was only pure spherical γ-Al_2O_3 particles in the sample.

Trimm and Stanislaus [2] have summarized the controlling of the pore size in alumina. They showed that the micropores in alumina are originated from spaces within the particle, which are caused, for example, by the removal of the water from between the crystal planes. In addition, the mesopores in the alumina are related to the following factors. First is the size, shape and packing type of the primary particles. The other one is the size of the secondary particles. On the basis of these concepts and the results of XRD, TEM and nitrogen adsorption and desorption, we conclude that the micropores appearing in the samples calcined at 350 and 450°C, respectively, are originated from the spaces within the particles due to dehydration between the crystal planes of the pseudoboehmite. When the temperature was increased to 550°C, the phase transformation from pseudoboehmite to γ-Al_2O_3 was complete, and there was only the pure γ-Al_2O_3 phase in the sample. In other words, the micropores disappeared too.

As for the mesopores, the results of TEM show that there are spherical particles existing in the alumina calcined at 450°C, so it is reasonable to suggest that the mesopores in the sample come from the packing of these spherical particles. Because the γ-Al_2O_3 phase is not clear at 350°C (Fig. 11), thus there are few spherical particles. Therefore, there is only a little mesopore volume. Considering that there are also needle-like pseudoboehmite particles existing in the samples calcined at 450°C, therefore, the materials do not exhibit a uniform mesoporous distribution. When the temperature was increased to 550°C, the texture which consisted of the spherical γ-Al_2O_3 particles occurred in the final material. This result is in accordance with the work reported by Ismagilov et al. [24]. They showed that calcination of aluminum hydroxide granules in the temperature range of 500–600°C produced spherical γ-Al_2O_3. In our study, the size of these spherical particles is similar because the precursor sol has a uniform particle diameter distribution. Therefore, the voids, which come from the regular packing of these spherical particles, form the uniform mesopores at 550°C.

This result indicates that the formation of uniform mesopores is related to the morphology of the particles. Thus, preparation of the sols that have a uniform particle diameter distribution is not the only factor to be considered during the preparation of the materials with uniform pore size distribution from the sol–gel process, but the crystalline phase of the materials and the particle morphology are also factors need to be pondered.

4. Conclusion

A novel sol–gel process has been developed, in which the alumina sol can be prepared at room temperature from inorganic salts. This novel sol–gel process can be used to prepare uniform mesoporous aluminas. The application of ultrasonic treatment to provide energy instead of heating is one of the important factors to obtain a stable sol at room temperature. It is shown that the ultrasonic treatment exerts influence on the particle diameter distribution and the pH value of the sol. Additionally, ultrasonic treatment for10 min is found to be the best treating time. ^{27}Al NMR characterization shows that $Al_{13}{}^{7+}$ species exists in the alumina sols, and short-range repulsion between these $Al_{13}{}^{7+}$ species provides an extra force to make the sols to become stabilized at higher pH values. The role of the acid in this work is not only for peptizing, but also for reacting with amorphous aluminum hydroxide to produce the $Al_{13}{}^{7+}$ polymer. This is the most important reason why the $[H^+]/[Al^{3+}]$ ratios used are different for preparing sols under different concentrations. Based on the results of the characterizations of ^{27}Al NMR, DTA and XRD, a formation mechanism of the alumina sol is suggested. This mechanism explains quite well some new phenomena exhibited by these alumina sols.

The results of TEM show that the morphology of the particles changes with the calcination temperature. The morphology of the particles is spherical in the sol system. If the calcination temperature is 450°C, needle-like and spherical particles exist together. When the temperature is increased to 550°C, there are only pure spherical particles in the resulting material. The results of N_2 adsorption–desorption experiments show that micropores and mesopores exist in the alumina when calcined at 350 and 450°C, respectively. After calcined at 550°C, the alumina exhibits uniform mesoporous distribution. These uniform mesopores

are formed from the voids which are originated from the regular packing of the spherical particles. Therefore, the results of this work imply that the pore size distribution of the alumina is related to its crystalline phase and the morphology of the particles.

Acknowledgements

We are grateful to Ms. Xiumei LIU for acquiring the NMR spectra from DRX 400. The financial supports of the Chinese Academy of Sciences (No. KJ951-Al-508) and Research Institute of Petroleum Processing SINOPEC (No. X599007) are also acknowledged.

References

[1] S. Biz, M.L. Occelli, Catal. Rev.-Sci. Eng. 40 (3) (1998) 330.
[2] D.L. Trimm, A. Stanislaus, Appl. Catal. 21 (1986) 215.
[3] C.J. Brinker, D.M. Smith, R. Deshpande, P.M. Davis, S. Hietala, G.C. Frye, C.S. Ashley, R.A. Assink, Catal. Today 14 (1992) 155.
[4] B.E. Yoldas, J. Mater. Sci. 10 (1975) 1856.
[5] B.E. Yoldas, Am. Ceram. Soc. Bull. 54 (3) (1975) 289.
[6] K. Maeda, F. Mizukami, M. Watanabe, N. Arai, M. Toba, J. Mater. Sci. Lett. 9 (1990) 522.
[7] T. Lopez, A. Romero, A. Chavela, L. Razo, R. Gomez, React. Kinet. Catal. Lett. 43 (1991) 307.
[8] J.D.F. Ramsay, S.R. Daish, C.J. Wright, Faraday Discuss. Chem. Soc. 65 (1978) 65.
[9] B.E. Yoldas, J. Appl. Chem. Biotechnol. 23 (1973) 803.
[10] S. Roberts, J. McCaffrey, L. Giannuzzi, S. Roberts, F. Stevie, N. Zaluzec, in: X.F. Zhang, Z. Zhang (Eds.), Progress in Transmission Electron Microscopy. I. Concepts and Techniques, Tsinghua University Press, Springer, Berlin, 1999, Chapter 10, p. 353.
[11] A.W. Li, H.B. Zhao, J.H. Gu, G.X. Xiong, Chin. Sci. Bull. 142 (1997) 791.
[12] S.M. Bradley, R.A. Kydd, R.F. Howe, J. Coll. Interface Sci. 159 (1993) 405.
[13] W.O. Parker Jr., I. Kiricsi, Appl. Catal. A: Gen. 121 (1995) L7.
[14] C.J. Brinker, G.W. Scherer, Sol–gel Science: The Physics and Chemistry of Sol–Gel Processing, Academic Press, New York, 1990, Chapter 2, p. 61.
[15] W.L. Olson, L.J. Bauer, Better ceramics through chemistry II, in: C.J. Brinker, D.E. Clark, D.R. Ulrich (Eds.), Proceedings of the Material Research Society Symposium, Pittsburgh, PA, 1986, Vol. 73, p. 187.
[16] E. Morgado Jr., Y.L. Lam, S.M.C. Menezes, L.F. Nazar, J. Coll. Interface Sci. 176 (1995) 432.
[17] B.C. Lippens, J.J. Steggerda, in: B.G. Linsen (Ed.), Physical and Chemical Aspects of Adsorbents and Catalysts, Academic Press, London, 1970.
[18] S.S. Kenneth, H.A. David, C.E. Raymond Jr., J. Am. Chem. Soc. 108 (1986) 5641.
[19] R. Feng, H.M. Li, Sonochemistry and its Application, Anhui Science & Technology Press, China, 1992, pp. 1–25.
[20] T. Ono, Y. Ohguchi, O. Togari, Stud. Surf. Sci. Catal. 16 (1983) 631.
[21] R.S.H. Mikhail, S. Brunauer, E.E. Bodor, J. Coll. Interface Sci. 26 (1968) 45.
[22] S. Cabrera, J.E. Haskouri, J. Alamo, A. Beltran, D. Beltran, S. Mendioroz, M.D. Marcos, P. Amoros, Adv. Mater. 11 (5) (1999) 379.
[23] S.A. Bagshaw, T.J. Pinnavaia, Angew. Chem. Int. Ed. Engl. 35 (10) (1996) 1102.
[24] Z.R. Ismagilov, M.N. Shepeleva, R.A. Shkrabina, V.B. Fenelonov, Appl. Catal. 69 (1991) 65.